

Induced Focusing of Optical Beams in Self-Defocusing Nonlinear Media

Govind P. Agrawal

The Institute of Optics, University of Rochester, Rochester, New York 14619

(Received 26 January 1990)

The novel phenomenon of induced focusing occurring in a self-defocusing nonlinear medium is discussed theoretically. Induced focusing of a weak optical beam occurs when it copropagates with an intense pump beam whose intensity peaks at a place different from that of the weak beam. The physical mechanism behind induced focusing is cross-phase modulation that couples the two beams. The conditions under which induced focusing can occur are discussed by solving numerically the coupled amplitude equations which incorporate the effects of diffraction, self-phase modulation, and cross-phase modulation.

PACS numbers: 42.65.Jx, 42.65.Bp

Self-focusing is a well-known nonlinear optical phenomenon.¹ It refers to the nonlinear process that not only counteracts against diffraction-induced natural spreading of an optical beam but also can contract it once the power exceeds a critical value. The physical mechanism behind self-focusing has its origin in the nonlinear refractive index, $n = n_0 + n_2 I$, that increases with the intensity I whenever $n_2 > 0$. Such an intensity dependence of the refractive index produces a converging wave front through the nonlinear phenomenon of self-phase modulation (SPM) as the beam propagates in the medium. The wave-front curvature depends on the beam intensity and can overcome the natural diverging tendency of the beam for sufficiently intense beams. The beam is then said to be self-focused. For nonlinear media with $n_2 < 0$, SPM imposes a diverging wave front: Optical beams then spread faster than diffraction, and are said to self-defocus.

One may ask if an optical beam can be focused, at least partially, in a self-defocusing medium by copropagating it with another intense beam. Although somewhat counterintuitive, I show in this Letter theoretically that such a behavior is indeed possible under certain conditions. It is referred to as induced focusing because focusing is induced by the copropagating intense beam which itself experiences self-defocusing. The physical mechanism behind induced focusing is cross-phase modulation (XPM), a nonlinear effect through which the phase of an optical beam is affected by other copropagating beams.² XPM introduces a mutual coupling between the optical beams. Even though such a coupling does not lead to any energy transfer, XPM can redistribute the energy within each beam. It will be seen later that induced focusing results from such XPM-induced redistribution of the electromagnetic energy within the beam profile. Induced focusing has been recently discussed in the case of self-focusing media³⁻⁶ but has not attracted much attention in the context of self-defocusing. Induced focusing of self-defocusing optical beams is a novel, intriguing effect. The results presented in this Letter

indicate that it should be possible to observe it experimentally.

The mathematical description of the XPM-induced interaction between the two copropagating cw or quasi-cw beams is provided by the coupled amplitude equations which, in the paraxial approximation, take the form

$$\frac{\partial A_1}{\partial z} - \frac{i}{2k_1} \left(\frac{\partial^2 A_1}{\partial x^2} + \frac{\partial^2 A_1}{\partial y^2} \right) = \frac{ik_1 n_2}{n_{01}} (|A_1|^2 + 2|A_2|^2) A_1, \quad (1)$$

$$\frac{\partial A_2}{\partial z} - \frac{i}{2k_2} \left(\frac{\partial^2 A_2}{\partial x^2} + \frac{\partial^2 A_2}{\partial y^2} \right) = \frac{ik_2 n_2}{n_{02}} (|A_2|^2 + 2|A_1|^2) A_2, \quad (2)$$

where A_j is the slowly varying envelope amplitude, $k_j = 2\pi n_{0j}/\lambda_j$, and n_{0j} is the linear refractive index at the carrier wavelength λ_j ($j=1$ and 2). The nonlinearity coefficient n_2 , sometimes called the Kerr coefficient, is negative for a self-defocusing medium. For atomic media n_2 becomes negative on the low-frequency side of the absorption peak. In obtaining Eqs. (1) and (2), the nonlinear medium is taken to be homogeneous and stationary. Absorption is neglected but can easily be included. The last two terms on the right-hand side of Eqs. (1) and (2) are due to SPM and XPM, respectively. These equations are similar to those describing pulse propagation in optical fibers² where the diffraction terms are replaced by a dispersion term containing $\partial^2 A_j / \partial t^2$. They can also be thought of as the coupled nonlinear Schrödinger equations in two spatial transverse dimensions.

It is not easy to solve Eqs. (1) and (2) analytically, and a numerical approach is often necessary. Even numerical solutions require considerable computing resources when both x and y derivatives are included in Eqs. (1) and (2). However, considerable insight can be

gained by limiting diffractive coupling to one transverse dimension by setting $\partial A_j/\partial y = 0$ for $j=1$ and 2. This assumption is justified for nonlinear interaction in planar optical waveguides. It is expected to provide a qualitative description even for bulk nonlinear media and can be used, provided one is aware of its limitations. It is useful to introduce the normalized variables

$$X = \frac{x}{w_0}, \quad \xi = \frac{z}{L_D}, \quad U_j = \frac{A_j}{I_1^{1/2}}, \quad (3)$$

where $L_D = k_1 w_0^2$, and write Eqs. (1) and (2) in the form

$$\frac{\partial U_1}{\partial \xi} - \frac{i}{2} \frac{\partial^2 U_1}{\partial X^2} = \text{sgn}(n_2) i N^2 (|U_1|^2 + 2|U_2|^2) U_1, \quad (4)$$

$$\frac{\partial U_2}{\partial \xi} - \frac{i}{2} \frac{\lambda_2}{\lambda_1} \frac{\partial^2 U_2}{\partial X^2} = \text{sgn}(n_2) \frac{\lambda_1}{\lambda_2} i N^2 (|U_2|^2 + 2|U_1|^2) U_2. \quad (5)$$

The nonlinear interaction is described in terms of a single parameter N defined by

$$N = k_1 w_0 (|n_2| I_1 / n_{01})^{1/2}, \quad (6)$$

where w_0 is the spot size and I_1 is the peak intensity for the beam at the carrier wavelength λ_1 . The parameter L_D in Eq. (3) has the physical meaning of the diffraction length or the Rayleigh range.

Equations (4) and (5) are solved numerically by using the split-step Fourier method.⁷ The initial field distribution at $\xi=0$ depends on the spatial profiles of the two beams. If we assume that the probe and pump beams are initially Gaussian with the $1/e$ half-widths w_0 and w_0' , respectively, the initial conditions are

$$U_1(0, X) = \exp \left[- \left(\frac{w_0}{w_0'} \right)^2 \frac{X^2}{2} \right], \quad (7)$$

$$U_2(0, X) = \left(\frac{I_2}{I_1} \right)^{1/2} \exp \left[- \frac{(X - X_0)^2}{2} \right], \quad (8)$$

where $X_0 = x_0/w_0$ and x_0 is physical distance between the beam centers for the general case in which the two beams do not overlap completely. In the following discussion, a pump-probe configuration is considered by assuming that the probe beam at λ_2 is much less intense than the pump beam at λ_1 ($I_2/I_1 = 10^{-4}$). The pump intensity I_1 is chosen such that the parameter $N=5$. The parameter n_2 is chosen negative to correspond to a self-defocusing medium. The wavelength ratio is $\lambda_2/\lambda_1 = 0.9$. The initial width is taken to be the same for both beams ($w_0 = w_0'$). The parameter X_0 is varied in the range 0–2.

Consider first the case of completely overlapping pump and probe beams ($X_0=0$). Numerical solutions of Eqs. (4) and (5) show that both beams defocus as they propagate inside the nonlinear medium. Self-defocusing of the pump beam is expected as the probe is too weak to influence it. The probe profile is distorted significantly

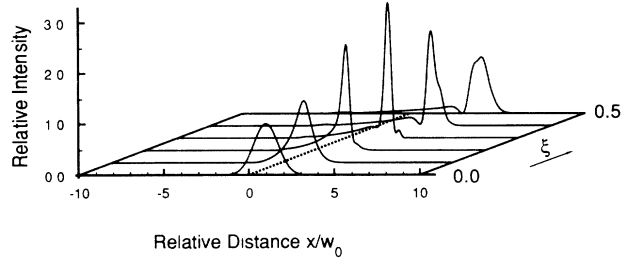


FIG. 1. Evolution of probe-beam profiles over a distance $\xi=0-0.5$ in a self-defocusing medium ($n_2 < 0$) for the case in which the probe copropagates with a pump beam of peak intensity such that $N=5$. The input beams are Gaussian, have the same width w_0 , and are separated by w_0 .

as a result of the XPM-induced coupling with the intense pump beam.⁶ However, the probe beam continues to spread, as expected, for $n_2 < 0$.

The situation changes completely when the centers of the two beams are allowed to be physically separated so that the beams overlap only partially at $\xi=0$. Figure 1 shows the probe evolution over the range $\xi=0-0.5$ for the case $X_0=1$. The probe beam exhibits a complex evolution pattern. In particular, it focuses initially in the form of a narrow beam before it begins to defocus. The spot size at $\xi=0.5$ is not much different from the input spot size (if the relatively long tail on one side is ignored). By contrast, the probe would be nearly 20 times wider than the input beam if $X_0=0$. As mentioned above, the initial contraction of the probe beam is due to pump-induced focusing occurring as a result of the XPM interaction between the two beams. The pump beam itself exhibits self-defocusing as expected for $n_2 < 0$. Figure 2 shows the pump evolution over the same range ($\xi=0-0.5$) and should be compared with Fig. 1.

What is the origin of induced focusing? A clue comes from the fact that this phenomenon occurs only when the beam centers do not coincide. The pump beam distorts the phase profile of the probe through XPM. If we neglect diffraction for the moment, Eq. (5) can be readily solved to obtain the XPM-induced phase shift ϕ_{NL} imposed on the probe by the pump. Neglecting a small SPM contribution, ϕ_{NL} is given by

$$\phi_{NL}(\xi, X) = -2N^2(\lambda_1/\lambda_2)e^{-X^2\xi}, \quad (9)$$

where $n_2 < 0$ was taken. As expected, XPM imposes a diverging wave front on the probe beam, and the probe indeed defocuses if its intensity profile peaks at the same location as the phase profile. However, when the probe-beam center is shifted from that of the pump beam, the intensity and phase profiles of the probe no longer peak at the same location. This mismatch leads to induced focusing. The physical mechanism can be understood by noting that the phase-front curvature $\partial^2 \phi_{NL}/\partial X^2$ becomes negative for $|X| > 1/\sqrt{2}$. The portion of the

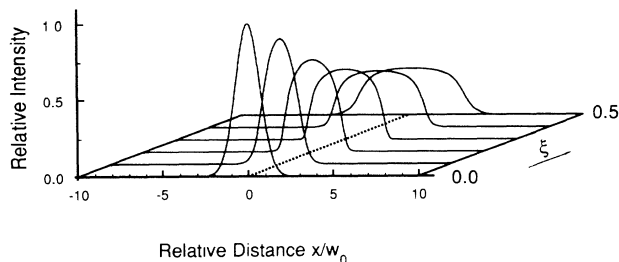


FIG. 2. Evolution of pump-beam profiles under same conditions as Fig. 1. The pump beam exhibits self-defocusing as expected for a nonlinear medium with $n_2 < 0$.

probe beam contained in that region focuses simply because of the negative phase-front curvature associated with it. This description is oversimplified as it ignores the effect of pump diffraction and defocusing. As the pump beam defocuses (see Fig. 2), the XPM-induced phase profile changes continuously as it mimics the pump-intensity profile. Eventually, the phase-front curvature becomes positive over the entire probe beam. This is the reason why the probe begins to defocus in Fig. 1 for $\xi > 0.4$. This is also the reason why the probe peak shifts toward the right in Fig. 1 as ξ increases.

Figure 1 is obtained for a specific value of the pump intensity ($N=5$) and a specific ratio of the pump-probe spot sizes ($w_0 = w'_0$). For such a pump beam the probe spot size is reduced by about a factor of 4 near $\xi=0.3$ compared with the input spot size [comparison is being made on the basis of the full width at half maximum (FWHM)]. Larger reduction factors are possible for higher pump intensities so that the parameter N given by Eq. (6) is larger. The intensity profile of the focused probe is also quite sensitive to the initial pump-probe spot sizes and the initial separation between the beam centers.

One may ask if it is possible to realize induced focusing for the case in which the pump and probe beams are not physically separated at the input end of the nonlinear medium. It turns out that this is indeed possible, provided the pump- and probe-intensity profiles are different from each other in such a way that the pump intensity is minimum at the peak of the probe intensity. For example, the pump-intensity distribution may correspond to a higher-order Gaussian beam. The higher-order Gaussian beams have been extensively studied and are described by the Hermite-Gauss functions in the rectangular geometry and by the Laguerre-Gauss functions in the cylindrical geometry.⁸ They can be realized in practice by using lasers which are forced to oscillate in higher-order transverse electromagnetic (TEM) modes. For illustration, we consider the case in which the probe and pump beams correspond to TEM₀₀ and TEM₁₁ modes, respectively. Restricting ourselves to only one transverse dimension, Eqs. (4) and (5) are now solved with the ini-

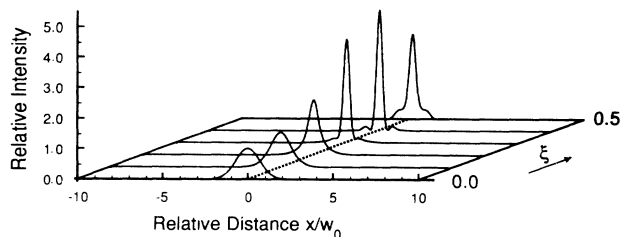


FIG. 3. Evolution of probe-beam profiles over a distance $\xi=0.5$ for the case in which the pump beam corresponds to a higher-order Gaussian beam. The other parameters remain the same.

tial condition

$$U_1(0, X) = \frac{1}{2} X \exp(-X^2/8), \tag{10}$$

$$U_2(0, X) = (I_2/I_1)^{1/2} \exp(-X^2/2), \tag{11}$$

where we assumed $w'_0 = 2w_0$. The pump profile (10) has zero intensity at $X=0$, where the probe intensity is maximum. The pump intensity peaks off center at $X = \pm 2$.

Figure 3 shows the probe evolution over the range $\xi=0-0.5$ by using parameter values identical to those of Fig. 1 but with the pump profile of Eq. (10). The probe beam exhibits induced focusing through the same mechanism (XPM), but the evolution pattern is quite different. In particular, the probe profile remains symmetric and exhibits a narrow peak at $x=0$. The maximum narrowing occurs near $\xi=0.35$ beyond which the probe begins to defocus. Figure 4 compares the focused probe beam at $\xi=0.35$ with the input Gaussian beam at $\xi=0$. The FWHM of the focused beam is smaller by more than a factor of 4 than the input FWHM. Note also a small pedestal around the focused beam; it contains the power that could not be focused by the XPM-

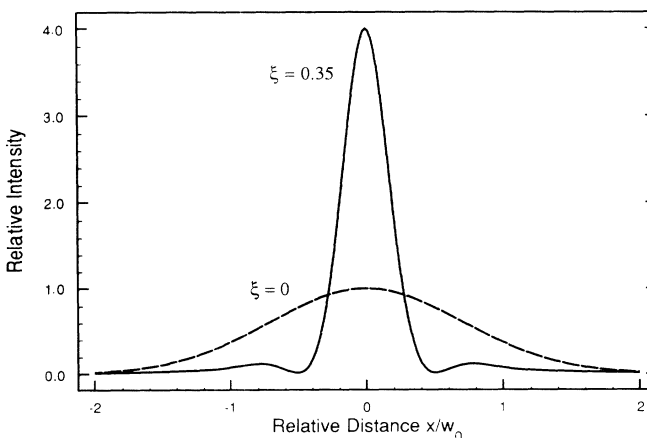


FIG. 4. Comparison of the probe-beam profile at $\xi=0.35$ with the input profile at $\xi=0$ showing induced focusing for the case of Fig. 3.

induced interaction between the pump and probe beams. The amount of power contained in the pedestal is sensitive to the ratio w'_0/w_0 and can be minimized by optimizing it. The origin of induced focusing is related to the negative curvature of the pump-induced phase profile. For the pump field of Eq. (10) the curvature is negative over the region $|X| \leq 2$. Since most of the probe energy is contained in that region, only a small amount of probe energy appears in the pedestal seen in Fig. 4.

Induced focusing described here should be observable experimentally by using common nonlinear media for which $n_2 < 0$. This is the case when the pump wavelength λ_1 is tuned on the long-wavelength side of a resonant absorption line, modeled as a two-level system. An atomic vapor such as sodium can be used together with a dye laser that provides the pump beam. For a 100- μm spot-size pump beam, $N=5$ can be realized if the nonlinear index change $|n_2|I_1 \sim 10^{-5}$. Depending on the value of n_2 , the peak intensity $I_1 \sim 1-100 \text{ MW/cm}^2$ is required. Such intensities are readily available, particularly if the Q -switched pulses are used. The steady-state theory developed here is applicable for such pulses if the medium response time is much shorter than the pulse duration. Since the diffraction length $L_D \sim 10 \text{ cm}$ for a 100- μm spot-size pump beam, induced focusing can be observed by using samples only a few centimeters long.

In conclusion, this Letter has discussed the novel phenomenon of induced focusing occurring in self-defocusing nonlinear media as a result of XPM. When a weak optical beam copropagates with an intense pump beam, the XPM-induced interaction between the two beams can focus the weak beam, even though the pump beam exhibits self-defocusing. Induced focusing occurs whenever the intensities of the two input beams peak at different locations. We have discussed the physical

mechanism and indicated how induced focusing can be observed experimentally. The results obtained here also apply to pulse propagation in nonlinear dispersive media such as optical fibers. They suggest that weak optical pulses can be compressed in the normal-dispersion regime by copropagating them with suitably shaped pump pulses. This conclusion is important for the field of ultrafast phenomena.

It is a pleasure to acknowledge helpful discussions with R. W. Boyd and C. J. McKinstrie. This research is supported by the U.S. Army Research Office and the Joint Services Optics program.

¹For a review, see, for example, Y. R. Shen, *The Principles of Nonlinear Optics* (Wiley, New York, 1984), Chap. 17, p. 303; see also J. H. Marburger, *Prog. Quantum Electron.* **4**, 35 (1975).

²For a review and related references, see G. P. Agrawal, *Nonlinear Fiber Optics* (Academic, Boston, 1989), Chap. 7; see also *The Supercontinuum Laser Source*, edited by R. R. Alfano (Springer-Verlag, New York, 1989), Chap. 4.

³C. J. McKinstrie and D. A. Russell, *Phys. Rev. Lett.* **61**, 2929 (1988).

⁴P. L. Baldeck, F. Raccah, and R. R. Alfano, *Opt. Lett.* **12**, 588 (1987).

⁵A. B. Grudinin, E. M. Dianov, D. V. Korbkin, A. M. Prokhorov, and D. V. Khaidarov, *Pis'ma Zh. Eksp. Teor. Fiz.* **47**, 297 (1988) [*JETP Lett.* **47**, 356 (1988)].

⁶G. P. Agrawal, *J. Opt. Soc. Am. B* (to be published).

⁷The split-step Fourier method is also known as the beam-propagation method. See G. P. Agrawal, *Nonlinear Fiber Optics* (Ref. 2), Sec. 2.4, for a discussion of the numerical schemes.

⁸For example, see A. E. Siegman, *Lasers* (University Science Books, Mill Valley, CA, 1986), Chaps. 16 and 17.